Mausam, (1986), **37**, 2. 147-152

551.553.21 : 551.515.1

Effect of Ekman boundary layer friction on the baroclinic growth of monsoon depression

(MRS.) P. S. SALVEKAR and S. K. MISHRA

Indian Institute of Tropical Meteorology, Pune

(*Received 13 December 1984*)

सार — परिसीमा स्तर में परिवर्तनीय ऊर्ध्वाधर कर्तनियों पर माध्य मानसून क्षेत्रीय प्रवाह का रैखिक बैरोक्लिनिक स्थायित्व विश्लेषण किया गया है। इसके लिए एकमैन परिसीमा स्तर घर्षण के साथ एक रुद्धोष्म, भूविक्षेपी कल्प, 25 स्तर, आंकिक निदर्श का उपयोग किया गया है। यह पाया गया है कि एकमैन घर्षण लघु तरंग (शार्ट वेव) क्षेत्र ($L \leqslant 3000$ कि. मी.) में विकास दर कम कर देता है। ध्यान देने की बात है कि वरीय लघु तरंग के चयन में घर्षण एक महत्वपूर्ण भूमिका निभाता है।

घर्षण के प्रभाव का स्पष्ट रूप से पता लगाने के लिए श्यान तथा अश्यान तरंगों की ऊर्ध्वाधर संरचनाओं का अभिकलन किया गया है। निष्कर्ष यह निकला कि तरंग आयाम की ऊर्ध्वाधर संरचना पर घर्षण का प्रभाव बुनियादी पछुआ पवन अधिकतम से नीचे पवन कर्तनी के समानुपाती होगा। तरंग के ऊर्ध्वाधर झुकाव और ऊर्ध्वाधर विस्तार घर्षण के कारण बढ़ जाते हैं। इसके साथ ही यह भी देखा गया कि निम्न स्तरों पर घर्षण प्रत्यक्ष परिसंचरण पैदा कर देता है।

ABSTRACT. Linear baroclinic stability analysis of the mean monsoon zonal flow for varying vertical shear in the boundary layer is performed by using an adiabatic, quasi-geostrophic, 25-layer, numerical model with Ekman boundary layer friction. It is found that Ekman friction reduces the growth rates in the short wave region ($L \leqslant 3000$ km). It is important to note that the friction plays a crucial role in the selection of the short preferred wave.

In order to find the effect of friction explicitly, the vertical structures of the viscous and inviscid preferred waves are computed. It is concluded that the effect of friction on the vertical structure of wave amplitudes is proportional to the wind shear below the basic westerly wind maximum. The vertical tilts of the wave as well as vertical extension are increased due to friction. Further, it is noticed that the friction induces direct circulation in the lower layers.

1. Introduction

The atmospheric boundary layer is now being treated as an integral part of the atmospheric dynamics, so that the motions and transports of the boundary layer may be related to large scale dynamics. Ekman boundary layer friction is one of the important physical processes which is known to influence the development of monsoon disturbances. The role of baroclinic machanism in the formation of monsoon disturbances was established by Mishra and Salvekar (1980). Recently an attempt is made by Salvekar and Mishra (1985) to investigate the vertical structure and the energy processes of monsoon disturbances in the presence of Ekman boundary layer friction.

The effects of Ekman friction on the mid-latitude baroclinic unstable waves have been explored in great depth, but very few studies are available on the monsoonal zonal flow (Satyan *et al.* 1980, Dash and Keshavamurty 1982). The qualitative effects of Ekman friction on the monsoonal zonal flow can be understood from the effects noticed on the mid-latitude zonal flow but the quantitative effects cannot be visualised unless the experiment is repeated for the monsoonal zonal flow.

Vertical wind shear is an important parameter to determine baroclinic growth of unstable waves (Charney 1947). In this study main objective is to obtain the role of Ekman friction on the baroclinic growth and vertical structure of the short unstable waves depending on the wind shear in the boundary layer. Generally the top of the boundary layer is considered to be 900 mb. But in the tropical region during monsoon season, the depth of the boundary layer increases and reaches upto 850 mb. Therefore, in order to find the effect of friction depending on the wind shear, different vertical wind profiles below 850 mb are considered. Further, the effect of Ekman friction on the vertical structure and baroclinic energy conversions are obtained.

2. The basic state

The basic state parameters, zonal wind $\bar{u}$ and inverse static stability σ^{-1} which are the inputs of the model are obtained analytically by using the seasonal averaged

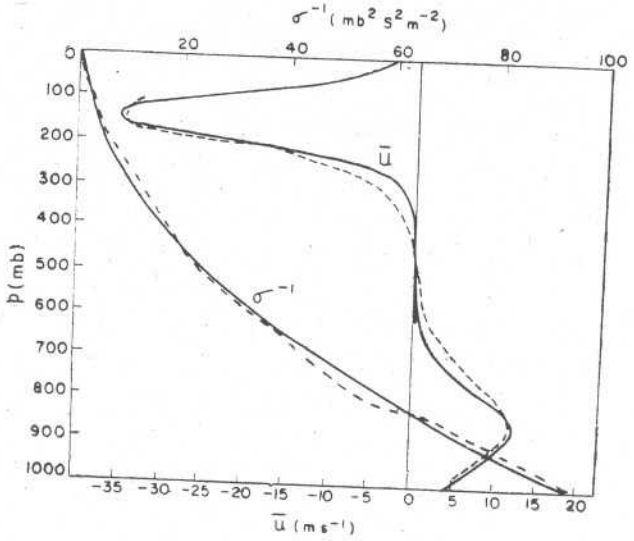

Fig. 1. Analytical (——) and observed (- - - -) vertical profiles of the mean zonal flow $\bar{u}$ and inverse static stability σ^{-1}

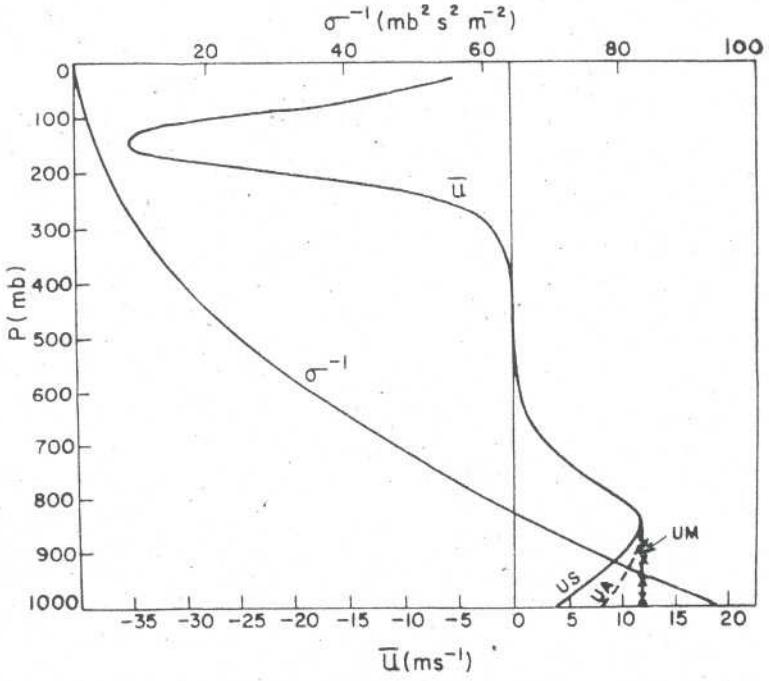

Fig. 2(a). Analytical vertical profiles of the basic states used in this study

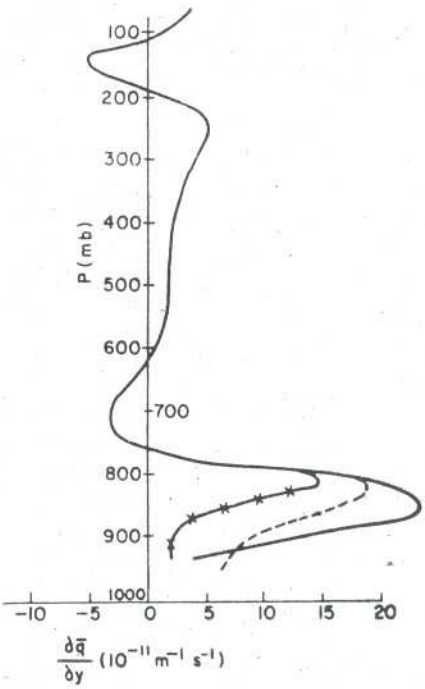

Fig. 2(b). Meridional gradient of potential vorticity for the basic states shown in Fig. 2(a)

wind and temperature fields. The analytical expressions for $\bar{u}$ and σ^{-1} are given as

$$\bar{u} = U_W \operatorname{sech}^2\left(\frac{p - P_W}{P_L}\right) - U_E \operatorname{sech}^2\left(\frac{p - P_E}{P_U}\right) \tag{2.1}$$

and

$$\sigma^{-1} = \begin{cases} ap^2 + b & \text{for } p > 140 \text{ mb} \\ a_* p + b_* & \text{for } p \leqslant 140 \text{ mb} \end{cases} \tag{2.2}$$

where U_W (12 ms^{-1}), U_E (35 ms^{-1}) and P_W (850 mb), P_E (140 mb) are the magnitudes and positions of the westerly and easterly maximum wind, respectively. The values of P_L (125 mb) and P_U (75 mb) are chosen such that they are related to the vertical half widths of the westerly and easterly parts of zonal flow. The empirical constants in the expression of σ^{-1} are chosen such that

$$a = 9.32 \times 10^{-5} \text{ m}^{-2} \text{ s}^2, \text{ and } b = 1.8 \text{ mb}^2 \text{ m}^{-2} \text{ s}^2,$$

$$a_* = 6.25 \times 10^{-3} \text{ mb m}^{-2} \text{ s}^2 \text{ and } b_* = .25 \text{ mb}^2 \text{ m}^{-2} \text{s}^2.$$

Using these constants in the expressions of $\bar{u}$ and σ^{-1} the analytical profiles are found to be close to the observed profiles (Fig. 1).

The analytical vertical profile of $\bar{u}$ obtained from the expression (2.1) is found to be symmetric w.r.t. both easterly and westerly maximum levels with surface wind value 4 ms^{-1} (hereafter this will be referred to as US). In order to consider different vertical wind shears in the boundary layer two additional cases were considered (*i*) Asymmetric flow with surface wind of 8 ms^{-1} (hereafter indicated as UA) and (*ii*) modified flow with uniform speed of 12 ms^{-1} from surface to 850 mb (hereafter indicated as UM). For constructing the UA profile from the expression (2.1) the parameter P_L is chosen to be 200 mb for $p \geqslant 850$ mb. The US, UA and UM profiles differ only below 850 mb. The US, UA, UM and the σ^{-1} profiles are shown in Fig. 2(a). In order to verify the necessary condition of baroclinic instability the meridional gradient of potential vorticity for the basic states as shown in Fig. 2(a) are computed and are presented in Fig. 2(b).

3. The numerical model

The governing equation of the model is the potential vorticity equation. It may be noted that generally numerical models are based on vorticity and thermodynamic energy equations and are shown to conserve the total energy. The atmosphere is divided into 25 layers in vertical each of uniform thickness in pressure ($\triangle p=$ 40 mb). Basic zonal flow and stream function are defined at the middle of layers while at the levels static stability is considered. The governing equation is applied at the middle of each layer using centred difference scheme for the pressure derivatives. At the top and bottom layer, vertical boundary conditions obtained from linearised form of thermodynamic energy equation are incorporated with the assumption that the basic zonal flow satisfies the condition of internal jet. The vertical boundary conditions of the model are obtained by considering $\omega=0$ at $p=0$ and $\omega=\omega_f$ at $p=1000$ mb, ω_f is the frictionally induced vertical velocity at the top of the boundary layer as proposed by Charney and Eliasen (1949), *i.e.*,

$$\omega_f = -g\rho\,(K/2f_0)^{\frac{1}{2}}\,(\nabla^2\psi)_{p_0}\,\sin 2\alpha$$

where $K\,(=4m^2\ s^{-1})$ is the eddy viscosity coefficient, $\alpha\,(=15°)$ is the cross isobar angle; g and ρ have their usual meanings. The Coriolis and Rossby parameters (f_0 and β) are considered at 17.5° N.

We consider perturbation as a single wave of zonal wave number $k = 2\pi/L$, L is the zonal wavelength and confined between two rigid walls separated by a distance D in the meridional direction. At the lateral boundaries the wave amplitude vanishes. To satisfy the lateral boundary condition the wave can be expressed as

$$A'(x, y, p, t) = \sin ly\,[A_1(p, t)\cos kx + A_2(p,\ t)\sin kx]$$

where A' stands for the stream function ψ', vertical velocity ω' and temperature T'. $l\,(=\pi/D)$ is the meridional wave number. An initial value approach is used to obtain the numerical solution. Time integration of the model is performed using Modified Euler Backward scheme for the first time step and Leap-frog scheme for the subsequent time steps. The time step is considered to be 1 hr. The time filter as suggested by Robert (1966) is used with a filter parameter as .01 in order to damp the computational modes.

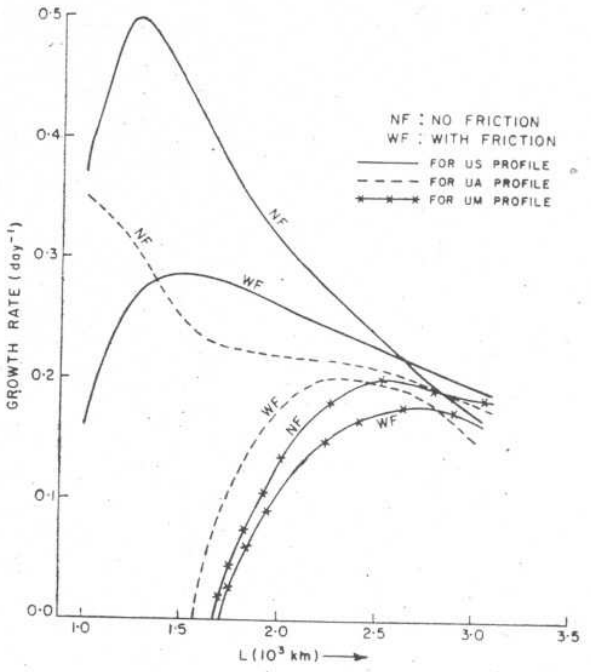

Fig. 3. Growth rate profiles for viscous (WF) and inviscid (NF) case in the shortwave region for US, UA and UM profiles

TABLE 1

Short preferred wave and growth rates of different $\bar{u}$ profiles, for $D=1500$ km

Cases	US	$\bar{u}$ UA	UM	Parameters
Inviscid	1250	—	2600	Preferred wavelength(km)
	.495	—	.19	Growth rate (day^{-1})
Viscous	1500	2250	2750	Preferred wavelength (km)
	.285	.208	.178	Growth rate (day^{-1})

4. The effect of Ekman boundary layer friction

4.1. *Growth rates of the viscous and inviscid waves*

Monsoon depressions have zonal wavelength about 2000-2500 km (Sikka 1977, Shukla 1978). Therefore, the wavelength band 1000 to 3000 km at an interval of 250 km was considered to find the effect of Ekman friction on the growth rates of the short unstable waves (of monsoon depression scale). The growth rate spectra for viscous and inviscid cases were obtained by considering different $\bar{u}$ profiles (US,UA and UM) and $D=1500$ km (Fig. 3). The short viscous preferred wavelengths for US and UM profiles are 1500 km and 2750 km respectively. These wavelengths are higher than corresponding wevelengths for inviscid cases, *viz.*, 1250 km and 2600 km respectively. It was already noticed that the growth rates of long waves are not affected by the low level westerlies (Mishra and Salvekar 1980) as well as by the Ekman friction (Salvekar 1984). Therefore, the growth rate spectra in Fig. 3 are presented for the short wavelengths only. It was found that the effect of Ekman friction on the growth rate is qualitatively similar to the effect noticed due to decrease of wind shear, *i.e.*, growth rate decreases and preferred wavelength increases (Table 1). The

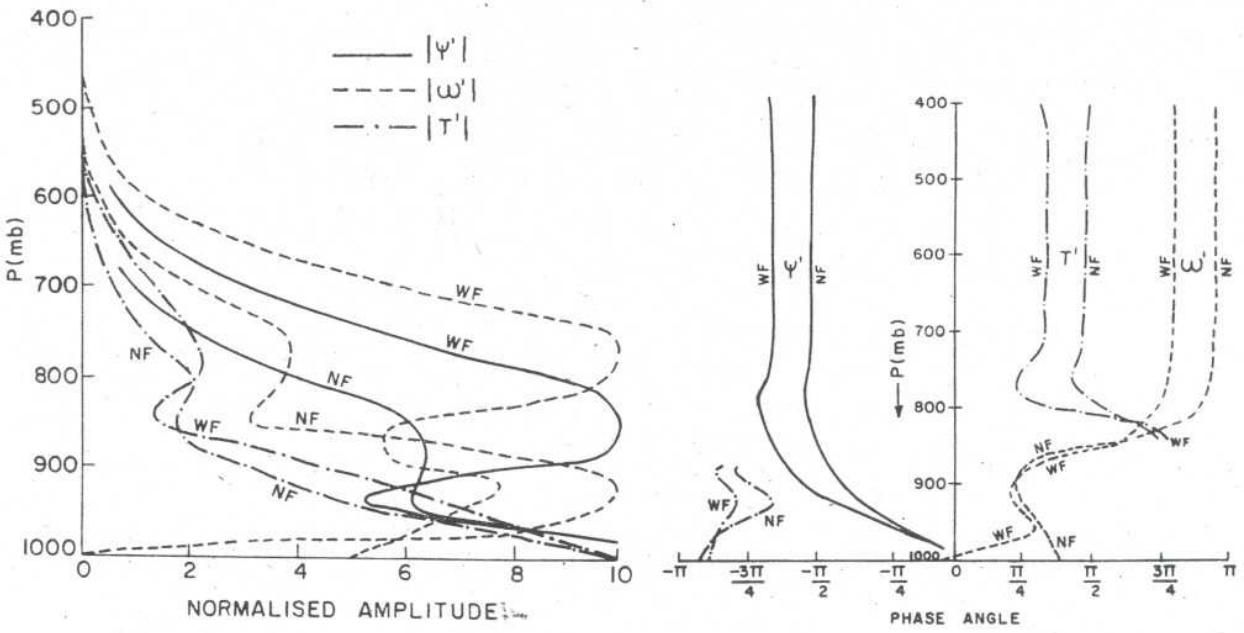

Figs. 4(a & b). Vertical profiles of the (a) normalised amplitudes and(b) phase angles of the ψ', ω' and T' fields for the viscous and inviscid preferred waves of US profile

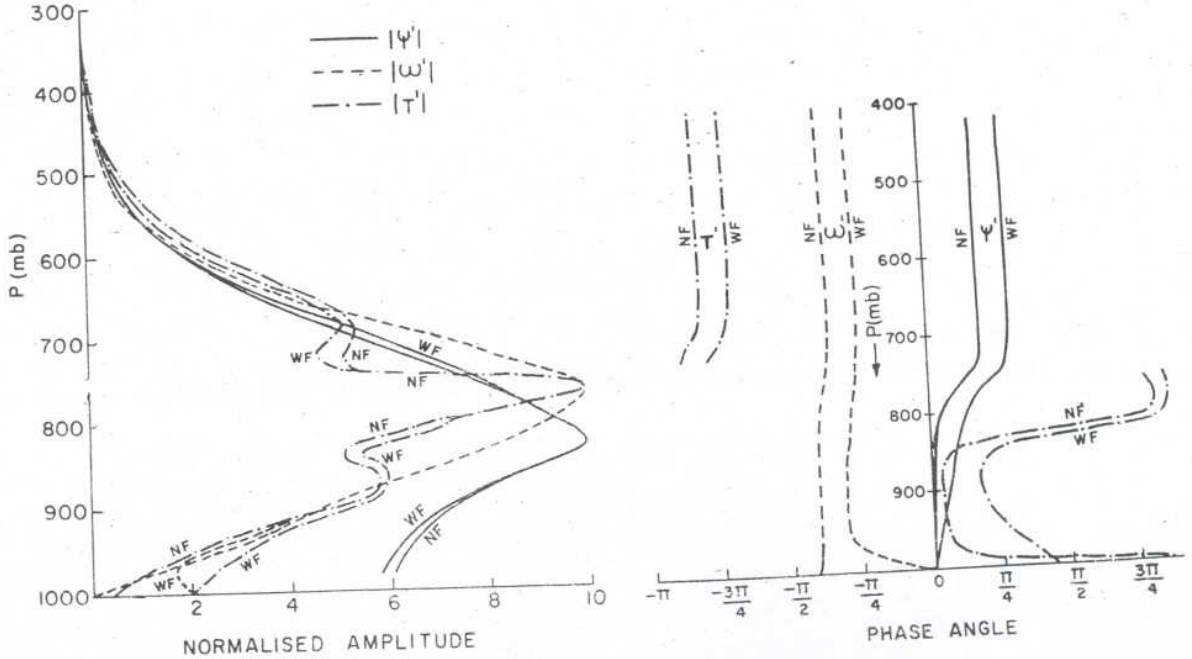

Figs. 5. (a & b). Same as Fig. 4 except for the preferred waves of UM profile

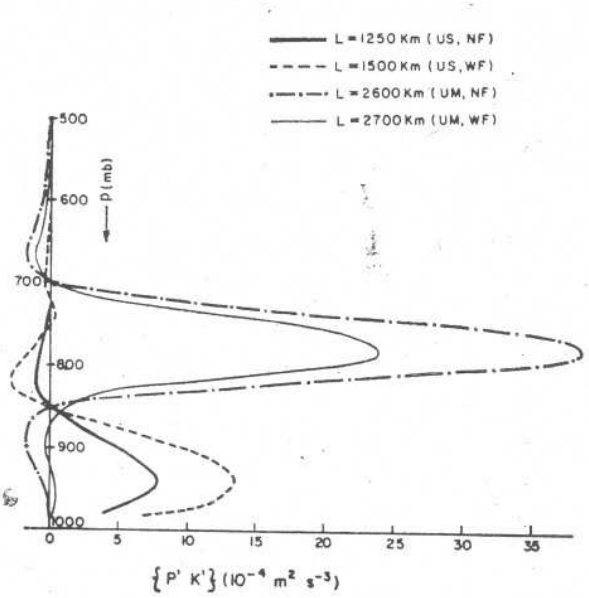

Fig. 6. Vertical profiles of $\{P'. K'\}$ for the viscous (WF) and inviscid (NF) preferred waves of US and UM wind profiles

decrease in the growth rates with the inclusion of Ekman friction was also noticed by Dash and Keshavamurty (1982). It may be noted that the growth rate spectra for UA profile in the presence of Ekman friction has a well defined peak which was not seen in the inviscid case. Such a difference between the viscous and inviscid growth rates was also pointed out by Dash and Keshavamurty (1982). Thus we may conclude that Ekman friction plays an important role in determining the zonal scale of the short unstable wave.

4.2. *Comparison between the vertical structures of the viscous and inviscid preferred waves*

Since the growth rate spectra for UA profile in the absence of boundary layer friction did not show the existence of a preferred wave, the other two zonal wind profiles, *namely*, US and UM were considered in this case for investigating the influence of boundary layer friction on the unstable modes. Vertical profiles of the perturbation stream function ψ', vertical velocity ω' and temperature T' of the preferred waves for the cases with friction (WF) and no friction (NF) were computed. The vertical profiles of the wave amplitudes and phase angles of all the fields are presented in Figs. 4 and 5. The amplitude values are normalised so that maximum value is 10 for each profile; the phase angles denote the position of wave trough. A comparison of the vertical structures of the inviscid and viscous preferred waves of the US profile (Fig.4) show significant changes as compared to the those of UM profile. The positions of primary and secondary maxima of $|\psi'|$ and $|\omega'|$ (Fig. 4a) of US profile get interchanged in the presence of boundary layer friction. This is due to decrease of wave amplitude in the lower levels due to friction. Changes in the $|T'|$ profile are much smaller than changes in $|\psi'|$ or $|\omega'|$ profiles. Further, the friction leads to more pronounced tilts (Fig. 4b) with height in all the three fields. These results are similar to those found by Card and Barcilon (1982) for mid-latitude westerly zonal wind profile with uniform vertical shear.

The influence of friction is almost insignificant on the amplitude distributions of UM profile (Fig. 5a). This may be due to the small wave amplitude at the surface which in turn implies small vertical velocity due to the Ekman pumping. The effect on wave tilt (Fig. 5b) is similar to that found for US profile. Thus it is concluded that the effect of friction is dependent on the basic zonal wind profile in the lower levels.

Examination of the phase difference between T' and ω' waves for US profiles presented in Fig. 4(b) leads to the conclusion that warm air is rising and cold air is sinking below 850 mb; *vice versa* above it. To confirm the lower level direct circulation and upper level indirect circulation we have computed the horizontally averaged baroclinic energy conversions. The vertical profiles of eddy available potential energy P' to eddy kinetic energy K', *i.e.*, $\{P'. K'\}$ for viscous and inviscid preferred waves are presented in Fig. 6. The positive (negative) values of $\{P'. K'\}$ indicate region of direct (indirect) circulation. By inclusion of friction the low level direct circulation is considerably intensified. In the case of UM profile, the lower layer indirect circulation is replaced by the direct circulation by inclusion of friction . This shows that friction induces direct circulation in the lower levels.

5. Conclusions

By performing the adiabatic, quasi-geostrophic, pure baroclinic, linear stability analysis of mean monsoon flow for varying vertical shear in the boundary layer, the effect of Ekman boundary layer friction on the growth rates and vertical structure of short unstable waves ($L \leqslant$ 3000 km) are studied. The growth rates in the short wavelength region are found to decrease with the decrease of wind shear below westerly maximum level as well as by inclusion of the boundary layer friction. The study leads to the conclusion that the Ekman friction plays a crucial role in the selection of the zonal preferred wave.

It is important to note that the effect of friction on the growth and vertical structure of short waves is qualitatively same as that obtained by Card and Barcilon (1982). The change in the vertical structure of the wave in the presence of Ekman friction depends on the wind shear below 850 mb. In other words, the effect of friction decreases with the decrease of wind shear below the westerly maximum level. The computations of vertical velocity and temperature distributions as well as baroclinic energy conversions indicate that the friction induces direct circulation in the lower levels.

Acknowledgements

The authors would like to thank Mrs. Leela George for preparation of the manuscript and to Miss S.M. Deshpande for typing it. They are extremely thankful

to Dr. Bh. V. Ramana Murty, Director for continuous support and encouragement and to Dr. R. Anantha-krishnan for his keen interest in this work.

References

Card, P.A. and Barcilon, A., 1982, *J. Atmos. Sci.*, **39**, 2128-2137.

Charney, J.G., 1947, *J. Met.*, **4**, 135-162.

Charney, J.G. and Eliasen, A., 1949, *Tellus*, **1**, 38-54.

Dash, S. K. and Keshavamurty, R. N., 1982, *Contribution to Atmos. Phys.*, **55**, 299-310.

Mishra, S.K. and Salvekar, P.S., 1980, *J. atmos, Sci.*, **37**, 389-394.

Robert, A.J., 1966, *J. Met. Soc. Japan*, **44**, 237-245.

Salvekar, P.S., 1984, Ph. D. Thesis (University of Poona).

Salvekar, P. S. and Mishra S. K., 1985, *Pageoph*, **123**, 3.

Satyan, V. *et al.*, 1980, *Indian Acad. Sci.* (E&P Sci.), **89**, 277-292.

Shukla, J., 1978, *J. Atmos. Sci.*, **35**, 495-508.

Sikka, D.R., 1977, *Pageoph*, **115**, 1501-1529.